
Numerical Simulation of a Molten Carbonate Fuel Cell by Partial Differential Algebraic Equations

K. Chudej¹, M. Bauer¹, H.J. Pesch¹, and K. Schittkowski²

¹ Lehrstuhl für Ingenieurmathematik, Universität Bayreuth, 95440 Bayreuth

² Fachgruppe Informatik, Universität Bayreuth, 95440 Bayreuth

Summary. The dynamical behavior of a molten carbonate fuel cell (MCFC) can be modeled by systems of partial differential algebraic equations (PDEAs) based on physical and chemical laws. Mathematical models for identification and control are considered as valuable tools to increase the life time of the expensive MCFC power plants, especially to derive control strategies for avoiding high temperature gradients and hot spots. We present numerical simulation results for a load change of a new one-dimensional counterflow MCFC model consisting of 34 nonlinear partial and ordinary differential algebraic-equations (PDEAs) based on physical and chemical laws. The PDAE system is discretized by the method of lines (MOL) based on forward, backward, and central difference formulae, and the resulting large system of semi-explicit differential-algebraic equations is subsequently integrated by an implicit DAE solver.

1 Introduction

Molten carbonate fuel cells (MCFCs) are a challenging new technology for stationary power plants, see e.g. Bischoff and Huppmann [2], Rolf [11], or Winkler [19]. They allow internal reforming of a fuel gas, for example methane, inside the cell with an operating temperature of about 650° C, and have the advantage of producing clean exhaust gases. The dynamical behavior of MCFCs can be modeled by one- and two dimensional systems of partial differential algebraic equations, see Heidebrecht and Sundmacher [8, 9, 10]. One of these particular models was recently validated for a real fuel cell operated at the power plant of the Magdeburg university hospital, see Gundermann, Heidebrecht, and Sundmacher [5].

The following main assumptions are made to derive the MCFC model equations, see also Heidebrecht [7]. First, plug flow conditions for the gas phase in anode and cathode are assumed, where different phases may have different temperatures and may exchange heat. All solid parts of the cell are lumped to one phase with respect to enthalpy balance. The temperatures of the two

gas phases are calculated separately, and the MCFC is operated at nearly ambient pressure. We do not consider pressure drops across the gas channels, i.e., isobaric conditions are assumed. All cells in the stack behave alike, so that the simulation of a single cell is sufficient taking insulation conditions at boundaries of neighboring cells into account. All chemical substances have the same heat capacity, which is independent of temperature. Reaction enthalpies are independent of the temperature. The temperature dependent chemical equilibrium constants and standard open circuit voltages are approximated by affine-linear functions. Ideal gas law is applied. Reforming reactions in the anode gas channel are modeled as quasi-homogeneous gas phase reactions using volume-related reaction rates. Methane steam reforming and water gas shift reactions are considered. Their heat of reaction is fully transferred to the gas phase. Diffusion in flow direction is negligible compared to convective transport. Heat exchange between electrode and gas phase is described by a linear function. The corresponding heat exchange coefficient also includes the effect of thermal radiation in a linearized form.

In this paper, we present a new one-dimensional counterflow model, see Bauer [1], which is derived from the two-dimensional crossflow model of Heidebrecht and Sundmacher [7, 10]. In contrast to a previous model presented in Chudej et al. [3], this new one has differential time index $\nu_t = 1$ and MOL index $\nu_{\text{MOL}} = 1$, which are easily derived from the two-dimensional analysis of Chudej, Sternberg, and Pesch [4]. The resulting dynamical system consists of twenty partial differential equations, four partial algebraic or steady-state equations, respectively, nine coupled ordinary differential and one coupled ordinary algebraic equation.

The spatial derivatives are approximated at grid points by forward, backward, and central difference formulae depending on the mathematical structure of the differential equation, especially the transport direction. An equidistant grid is used. Neumann boundary conditions are set for the heat equation and Dirichlet boundary conditions for the transport equations. Together with the additional coupled system of DAEs, the method of lines leads to a large set of differential algebraic equations, where the initial values are derived from the given initial values of the PDAE system. The procedure is called numerical method of lines, see Schiesser [12] or Schittkowski [15].

The nonlinear model equations are implemented in the model language PCOMP, see Schittkowski [17], under the interactive software system EASY-FIT, see Schittkowski [15, 16]. For a further set of practical PDAE models see Schittkowski [18].

Section 2 contains a brief summary of the technological background and the detailed mathematical equations. In Section 3, we describe the numerical procedures in more detail and present numerical simulation results for a load change of the fuel cell.

2 The Molten Carbonate Fuel Cell Model

2.1 Technological Description and Mathematical Variables

The model under investigation describes the dynamical behavior of a MCFC in a counterflow configuration with respect to anode and cathode gas streams, see Figure 1.

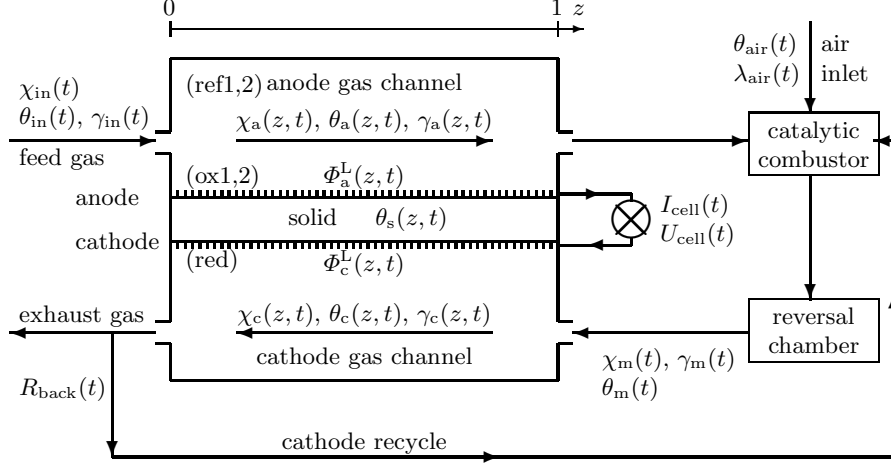
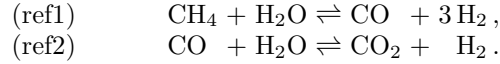
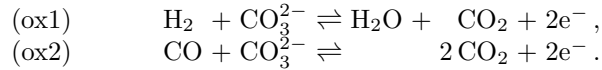


Fig. 1. 1D counterflow model of a molten carbonate fuel cell with mathematical variables and considered chemical reactions

In the anode channel, the feed gas, usually methane CH_4 , and water H_2O are converted to hydrogen H_2 , carbon monoxide CO , and carbon dioxide CO_2 , see Figure 1 (ref1, ref2). This reforming process consumes heat, and only high temperature fuel cells offer the opportunity for internal reforming.



Simultaneously, two electro-chemical reactions consume hydrogen and carbon monoxide to produce electrons in the porous anode electrode. Both consume carbonate ions, CO_3^{2-} , from the electrolyte layer which is located between the anode and cathode electrodes,



At the porous cathode electrode the reduction reaction produces new carbonate ions from oxygen, O_2 and carbon dioxide, CO_2 ,



Hereby, the carbonate ions produced at the cathode electrode are transferred through the electrolyte to the anode electrode. Electric current I_{cell} and cell voltage U_{cell} can be collected at the electrodes, see Figure 1.

The mathematical model uses the following mathematical variables, see again Figure 1, where $j \in \{\text{a, c, m, in}\}$:

- $\chi_{i,j}$ - molar fractions, $i \in I \stackrel{\text{def}}{=} \{\text{CH}_4, \text{H}_2\text{O}, \text{H}_2, \text{CO}, \text{CO}_2, \text{O}_2, \text{N}_2\}$,
- χ_j = $(\chi_{i,j})_{i \in I}$,
- γ_j - molar flow densities,
- θ_s - solid temperature,
- θ_j - gas temperatures,
- Φ_a^L, Φ_c^L - electrical potentials at anode and cathode,
- U_{cell} - cell voltage,
- I_{cell} - cell current,
- θ_{air} - temperature of air,
- λ_{air} - air number,
- R_{back} - cathode recycle switch.

The definition of molar fractions intrinsically leads to the balance equation $\sum_{i \in I} \chi_{i,j} \equiv 1$, $j \in \{\text{a, c, m, in}\}$, since the model equations fulfill $\sum_{i \in I} \frac{\partial \chi_{i,j}}{\partial t} \equiv 0$, $j \in \{\text{a, c}\}$. Therefore global minimal coordinates, i.e. a suitable subset of the molar fractions depending on the boundary conditions, can be applied.

The main variable is the solid temperature θ_s which is needed to define a heat equation. The solution of the solid temperature should avoid high temperature gradients and especially hot spots, which drastically shorten service life and eventually damage the fuel cell irreparably.

2.2 The Dynamical Model

All variables are dimensionless. One unit of the dimensionless time corresponds to 12.5 seconds. Input variable of the system is the cell current $I_{\text{cell}}(t)$, which is given as a step function for modeling a load change of the fuel cell.

For performing numerical simulations, the boundary conditions for the gas temperature θ_{in} , the molar fractions χ_{in} , and the molar flow density γ_{in} are given in form of time dependent functions at the anode inlet ($z = 0$). The quantities λ_{air} and θ_{air} are also prescribed as time dependent functions, see Figure 1.

Heat equation in the solid:

$$\frac{\partial \theta_s}{\partial t} = \lambda \frac{\partial^2 \theta_s}{\partial z^2} + f_1(\theta_s, \theta_a, \theta_c, \chi_a, \chi_c, \Phi_a^L, \Phi_c^L, U_{\text{cell}}), \quad \frac{\partial \theta_s}{\partial z} \Big|_{z \in \{0,1\}} = 0.$$

Advection equations in the gas streams:

$$\begin{aligned}\frac{\partial \chi_a}{\partial t} &= -\gamma_a \theta_a \frac{\partial \chi_a}{\partial z} + f_2(\theta_s, \theta_a, \chi_a, \Phi_a^L), & \chi_a|_{z=0} &= \chi_{\text{in}}(t), \\ \frac{\partial \chi_c}{\partial t} &= +\gamma_c \theta_c \frac{\partial \chi_c}{\partial z} + f_3(\theta_s, \theta_c, \chi_c, \Phi_c^L, U_{\text{cell}}), & \chi_c|_{z=1} &= \chi_{\text{m}}(t), \\ \frac{\partial \theta_a}{\partial t} &= -\gamma_a \theta_a \frac{\partial \theta_a}{\partial z} + f_4(\theta_s, \theta_a, \chi_a, \Phi_a^L), & \theta_a|_{z=0} &= \theta_{\text{in}}(t) \\ \frac{\partial \theta_c}{\partial t} &= +\gamma_c \theta_c \frac{\partial \theta_c}{\partial z} + f_5(\theta_s, \theta_c, \chi_c, \Phi_c^L, U_{\text{cell}}), & \theta_c|_{z=1} &= \theta_{\text{m}}(t).\end{aligned}$$

Steady-state equations for molar flow densities:

$$\begin{aligned}0 &= \frac{\partial(\gamma_a \theta_a)}{\partial z} - f_6(\theta_s, \theta_a, \chi_a, \Phi_a^L), & \gamma_a|_{z=0} &= \gamma_{\text{in}}(t), \\ 0 &= \frac{\partial(\gamma_c \theta_c)}{\partial z} - f_7(\theta_s, \theta_c, \chi_c, \Phi_c^L, U_{\text{cell}}), & \gamma_c|_{z=1} &= \gamma_{\text{m}}(t).\end{aligned}$$

Equations for potentials and current density:

$$\begin{aligned}\frac{\partial \Phi_a^L}{\partial t} &= [i_a(\theta_s, \chi_a, \Phi_a^L) - i]/c_a, \\ \frac{\partial \Phi_c^L}{\partial t} &= [i_a(\theta_s, \chi_a, \Phi_a^L) - i]/c_a + [i_e(\Phi_a^L, \Phi_c^L) - i]/c_c, \\ i &= (c_a^{-1} + c_e^{-1} + c_c^{-1})^{-1} \left(\frac{i_a - I_a}{c_a} + \frac{i_e - I_e}{c_e} + \frac{i_c - I_c}{c_c} \right) + I_{\text{cell}}\end{aligned}$$

Integro differential algebraic equations:

$$\begin{aligned}\frac{dU_{\text{cell}}}{dt} &= \frac{I_a - I_{\text{cell}}}{c_a} + \frac{I_e - I_{\text{cell}}}{c_e} + \frac{I_c - I_{\text{cell}}}{c_c} \\ I_a(t) &= \int_0^1 i_a(\theta_s, \theta_a, \chi_a, \Phi_a^L) dz, \\ I_c(t) &= \int_0^1 i_c(\theta_s, \theta_c, \chi_c, \Phi_c^L, U_{\text{cell}}) dz, \\ I_e(t) &= \int_0^1 i_e(\Phi_a^L, \Phi_c^L) dz, \\ \frac{d\chi_{\text{m}}}{dt} &= f_8(\theta_{\text{m}}, \chi_{\text{m}}, \theta_a|_{z=1}, \chi_a|_{z=1}, \gamma_a|_{z=1}, \theta_c|_{z=0}, \chi_c|_{z=0}, \gamma_c|_{z=0}, \\ &\quad \lambda_{\text{air}}, \theta_{\text{air}}, R_{\text{back}}), \\ \frac{d\theta_{\text{m}}}{dt} &= f_9(\theta_{\text{m}}, \theta_a|_{z=1}, \chi_a|_{z=1}, \gamma_a|_{z=1}, \theta_c|_{z=0}, \chi_c|_{z=0}, \gamma_c|_{z=0}, \\ &\quad \lambda_{\text{air}}, \theta_{\text{air}}, R_{\text{back}}), \\ \gamma_{\text{m}} &= f_{10}(\theta_{\text{m}}, \theta_a|_{z=1}, \chi_a|_{z=1}, \gamma_a|_{z=1}, \theta_c|_{z=0}, \chi_c|_{z=0}, \gamma_c|_{z=0}, \\ &\quad \lambda_{\text{air}}, \theta_{\text{air}}, R_{\text{back}}).\end{aligned}$$

Initial values:

$$\begin{aligned} \theta_s|_{t=0} &= \theta_{s,0}(z), \quad \theta_a|_{t=0} = \theta_{a,0}(z), \quad \theta_c|_{t=0} = \theta_{c,0}(z), \quad \theta_m|_{t=0} = \theta_{m,0}(z), \\ \chi_a|_{t=0} &= \chi_{a,0}(z), \quad \chi_c|_{t=0} = \chi_{c,0}(z), \quad \chi_m|_{t=0} = \chi_{m,0}(z), \\ \Phi_a^L|_{t=0} &= \Phi_{a,0}^L(z), \quad \Phi_c^L|_{t=0} = \Phi_{c,0}^L(z), \quad U_{\text{cell}}|_{t=0} = U_{\text{cell},0} \end{aligned}$$

Constraints:

$$\begin{aligned} \gamma_a &> 0, \quad \gamma_c > 0, \quad \theta_a > 0, \quad \theta_c > 0, \\ 0 &\leq \chi_{i,j} \leq 1, \quad i \in I, \quad j \in \{a, c, m, \text{in}\}, \\ \sum_{i \in I} \chi_{i,j} &\equiv 1, \quad j \in \{a, c, m, \text{in}\}. \end{aligned}$$

The dynamical behavior at the outlet of the reversal chamber is described by a DAE, which couples the outlet of the anode and the inlet of the cathode and, if the cathode recycle is switched on, with the outlet of the cathode. To summarize, we obtain a coupled PDAE/DAE system consisting of 34 nonlinear equations.

2.3 The Details

The missing functions are to be specified subsequently for the matter of completeness.

Right hand sides of the PDAEs:

$$\begin{aligned} f_1 &= - \sum_{\substack{i=\text{H}_2, \text{CO} \\ j=\text{ox}1,2 \\ \nu_{i,j} < 0}} (\theta_a - \theta_s) \nu_{i,j} Da_j r_j - \sum_{\substack{i=\text{CO}_2, \text{O}_2 \\ \nu_{i,\text{red}} < 0}} (\theta_c - \theta_s) \nu_{i,\text{red}} Da_{\text{red}} r_{\text{red}} \\ &\quad + q_{\text{solid}} - (\theta_s - \theta_a) St_{\text{as}} - (\theta_s - \theta_c) St_{\text{cs}}, \\ \frac{f_{2,i}}{\theta_a} &= \sum_{j=\text{ox}1,2,\text{ref}1,2} \left(\nu_{i,j} - \chi_{i,a} \sum_{k \in I} \nu_{k,j} \right) Da_j r_j, \\ \frac{f_4}{\theta_a} &= \sum_{\substack{i=\text{H}_2\text{O}, \text{CO}_2 \\ j=\text{ox}1,2 \\ \nu_{i,j} > 0}} (\theta_s - \theta_a) \nu_{i,j} Da_j r_j + \sum_{j=\text{ref}1,\text{ref}2} -\Delta_{\text{R}} h_j^0 \frac{Da_j r_j}{c_p} \\ &\quad + \frac{(\theta_s - \theta_a) St_{\text{as}}}{c_p}, \\ f_6 &= \frac{f_4}{\theta_a} + \theta_a \sum_{\substack{j=\text{ox}1,\text{ox}2,\text{ref}1,\text{ref}2 \\ i \in I}} \nu_{i,j} Da_j r_j, \\ \frac{f_{3,i}}{\theta_c} &= \left(\nu_{i,\text{red}} - \chi_{i,c} \sum_{j \in I} \nu_{j,\text{red}} \right) Da_{\text{red}} r_{\text{red}}, \end{aligned}$$

Table 1. Constants

c_p	4.5	F	$\frac{3.5}{8}$	λ	0.666/2.5	j	Da_j	Arr_j	θ_j^0	$\Delta_R h_j^0$	α_j^+	α_j^-	n_j
$c_{p,s}$	10000	κ_e	1	θ_u	1	ref1	25.0	84.4	2.93	90.5			
St_{as}	80.0	c_a	0.00001	λ_{air}	2.2	ref2	100.0	6.2	2.93	-14.5			
St_{cs}	120.0	c_e	0.00001	$\chi_{O_2,air}$	0.21	ox1	5.0	21.6	2.93	56.0	0.5		2.0
St_m	1.0	c_c	0.00001	θ_{air}	1.5	ox2	5.0	21.6	2.93	42.0	0.5		2.0
						red	0.3	31.6	2.93	156.0	2.5	0.5	2.0

i	$\Delta_C h_i^0$	$\nu_{i,ref1}$	$\nu_{i,ref2}$	$\nu_{i,ox1}$	$\nu_{i,ox2}$	$\nu_{i,red}$
CH ₄	-323.85	-1.0	0.0	0.0	0.0	0.0
H ₂ O	0.0	-1.0	-1.0	1.0	0.0	0.0
H ₂	-97.62	3.0	1.0	-1.0	0.0	0.0
CO	-114.22	1.0	-1.0	0.0	-1.0	0.0
CO ₂	0.0	0.0	1.0	1.0	2.0	-1.0
O ₂	0.0	0.0	0.0	0.0	0.0	-0.5
N ₂	0.0	0.0	0.0	0.0	0.0	0.0

$$\begin{aligned}
\frac{f_5}{\theta_c} &= \frac{St_{cs}}{c_p}(\theta_s - \theta_c), \quad f_7 = \frac{f_5}{\theta_c} + \theta_c \sum_{i \in I} \nu_{i,red} Da_{red} r_{red}, \\
i_a &= F \sum_{j=ox1,ox2} n_j Da_j r_j, \quad i_e = (\Phi_a^L - \Phi_c^L) \kappa_e, \\
i_c &= -F n_{red} Da_{red} r_{red}, \\
q_{solid} &= \sum_{j=ox1,ox2} [-\Delta_R h_j^0 + n_j (\Phi_a^S - \Phi_a^L)] Da_j r_j \\
&\quad + [-\Delta_R h_j^0 + n_{red} (\Phi_c^S - \Phi_c^L)] Da_{red} r_{red} + (\Phi_a^L - \Phi_c^L) i_e / F.
\end{aligned}$$

Reaction kinetics:

$$\begin{aligned}
r_{ref1} &= e^{Arr_{ref1} \left(\frac{1}{\theta_{ref1}^0} - \frac{1}{\theta_a} \right)} \cdot \left(\chi_{CH_4,a} \chi_{H_2O,a} - \frac{\chi_{H_2,a}^3 \chi_{CO,a}}{K_{ref1}} \right), \\
r_{ref2} &= e^{Arr_{ref2} \left(\frac{1}{\theta_{ref2}^0} - \frac{1}{\theta_a} \right)} \cdot \left(\chi_{CO,a} \chi_{H_2O,a} - \frac{\chi_{H_2,a} \chi_{CO_2,a}}{K_{ref2}} \right), \\
r_{ox1} &= e^{Arr_{ox1} \left(\frac{1}{\theta_{ox1}^0} - \frac{1}{\theta_s} \right)} \left[\begin{aligned} &\frac{\alpha_{ox1}^+ n_{ox1} (-\Phi_a^L - \Delta\Phi_{ox1}^0)}{\theta_s} \\ &\chi_{H_2,a} e \\ &\frac{-(1 - \alpha_{ox1}^+) n_{ox1} (-\Phi_a^L - \Delta\Phi_{ox1}^0)}{\theta_s} \\ &-\chi_{H_2O,a} \chi_{CO_2,a} e \end{aligned} \right],
\end{aligned}$$

$$r_{\text{ox2}} = e \quad Arr_{\text{ox2}} \left(\frac{1}{\theta_{\text{ox2}}^0} - \frac{1}{\theta_s} \right) \left[\begin{array}{l} \chi_{\text{CO},a} e \frac{\alpha_{\text{ox2}}^+ n_{\text{ox2}} (-\Phi_a^L - \Delta\Phi_{\text{ox2}}^0)}{\theta_s} \\ -\chi_{\text{CO}_2,a}^2 e \frac{-(1 - \alpha_{\text{ox2}}^+) n_{\text{ox2}} (-\Phi_a^L - \Delta\Phi_{\text{ox2}}^0)}{\theta_s} \end{array} \right].$$

$$r_{\text{red}} = e \quad Arr_{\text{red}} \left(\frac{1}{\theta_{\text{red}}^0} - \frac{1}{\theta_c} \right) \left[\begin{array}{l} \chi_{\text{CO}_2,c}^{-2} e \frac{\alpha_{\text{red}}^+ (U_{\text{cell}} - \Phi_c^L - \Delta\Phi_{\text{red}}^0)}{\theta_c} \\ -\chi_{\text{O}_2,c}^{0.75} \chi_{\text{CO}_2,c}^{-0.5} e \frac{-\alpha_{\text{red}}^- (U_{\text{cell}} - \Phi_c^L - \Delta\Phi_{\text{red}}^0)}{\theta_c} \end{array} \right].$$

$$K_{\text{ref1}}(\theta_a) = \exp(30.19 - 90.41/\theta_a), \quad K_{\text{ref2}}(\theta_a) = \exp(-3.97 + 14.57/\theta_a),$$

$$\Delta\Phi_{\text{ox1}}^0(\theta_s) = 28.26 - 19.84\theta_s, \quad \Delta\Phi_{\text{ox2}}^0(\theta_s) = 20.98 - 17.86\theta_s,$$

$$\Delta\Phi_{\text{red}}^0(\theta_s) = 78.00 - 23.06\theta_s.$$

Catalytic combustor and reversal chamber:

$$\gamma_{\text{air}} = \gamma_a|_{z=0} \frac{\lambda_{\text{air}}}{\chi_{\text{O}_2,a}|_{z=0}} (2\chi_{\text{CH}_4,a}|_{z=0} + 0.5\chi_{\text{CO},a}|_{z=0} + 0.5\chi_{\text{H}_2,a}|_{z=0})$$

$$\gamma_{\text{back}} = R_{\text{back}}(t)\gamma_c|_{z=0}$$

In the following equations $\theta_a, \chi_a, \gamma_a$ are abbreviations for $\theta_a|_{z=1}, \chi_a|_{z=1}, \gamma_a|_{z=1}$.

$$\gamma_b = \gamma_a \left(1 - \frac{1}{2}\chi_{\text{H}_2,a} - \frac{1}{2}\chi_{\text{CO},a} \right) + \gamma_{\text{air}} + \gamma_{\text{back}},$$

$$\chi_{\text{CH}_4,b} = \chi_{\text{H}_2,b} = \chi_{\text{CO},b} = 0,$$

$$\chi_{\text{H}_2\text{O},b} = \frac{\gamma_a}{\gamma_b} (2\chi_{\text{CH}_4,a} + \chi_{\text{H}_2\text{O},a} + \chi_{\text{H}_2,a}) + \frac{\gamma_{\text{back}}}{\gamma_b} \chi_{\text{H}_2\text{O},c}|_{z=0},$$

$$\chi_{\text{CO}_2,b} = \frac{\gamma_a}{\gamma_b} (\chi_{\text{CH}_4,a} + \chi_{\text{CO},a} + \chi_{\text{CO}_2,a}) + \frac{\gamma_{\text{back}}}{\gamma_b} \chi_{\text{CO}_2,c}|_{z=0},$$

$$\chi_{\text{O}_2,b} = \frac{\gamma_{\text{air}}}{\gamma_b} \chi_{\text{O}_2,\text{air}} - \frac{\gamma_a}{\gamma_b} \left(2\chi_{\text{CH}_4,a} + \frac{1}{2}\chi_{\text{H}_2,a} + \frac{1}{2}\chi_{\text{CO},a} \right) + \frac{\gamma_{\text{back}}}{\gamma_b} \chi_{\text{O}_2,c}|_{z=0},$$

$$\chi_{\text{N}_2,b} = \frac{\gamma_{\text{air}}}{\gamma_b} (1 - \chi_{\text{O}_2,\text{air}}) + \frac{\gamma_{\text{back}}}{\gamma_b} \chi_{\text{N}_2,c}|_{z=0},$$

$$\theta_b = \theta_u + \frac{\gamma_a}{\gamma_b} \left(\sum_{i \in I} \frac{-\Delta_c h_i^0}{c_p} \chi_{i,a} + \theta_a - \theta_u \right) + \frac{\gamma_{\text{air}}}{\gamma_b} (\theta_{\text{air}} - \theta_u)$$

$$+ \frac{\gamma_{\text{back}}}{\gamma_b} (\theta_c|_{z=0} - \theta_u),$$

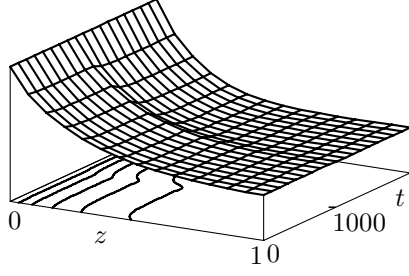


Fig. 2. Molar fraction $\chi_{\text{CH}_4,\text{a}}$ in anode gas channel

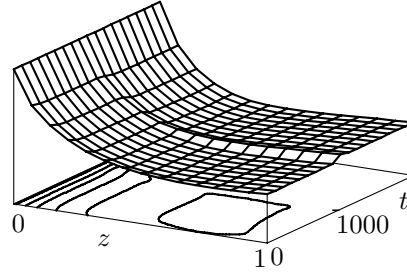


Fig. 3. Molar fraction $\chi_{\text{H}_2\text{O},\text{a}}$ in anode gas channel

$$\begin{aligned}
 f_{8,i} &= \gamma_b(\chi_{i,\text{b}} - \theta_{i,\text{m}})\theta_{\text{m}}, \\
 f_9 &= \gamma_b(\theta_{\text{b}} - \theta_{\text{m}})\theta_{\text{m}} - \frac{St_{\text{m}}}{c_p}(\theta_{\text{m}} - \theta_{\text{u}})\theta_{\text{m}}, \\
 f_{10} &= \gamma_b + \gamma_b \frac{\theta_{\text{b}} - \theta_{\text{m}}}{\theta_{\text{m}}} - \frac{St_{\text{m}}}{c_p} \frac{\theta_{\text{m}} - \theta_{\text{u}}}{\theta_{\text{m}}}.
 \end{aligned}$$

Non-zero boundary conditions:

$$\chi_{\text{CH}_4,\text{a}} = 1/3.5, \chi_{\text{H}_2\text{O},\text{a}} = 2.5/3.5, \theta_{\text{a}} = 3, \gamma_{\text{a}} = 1, R_{\text{back}} = 0.$$

Non-zero initial conditions at $t = 0$:

$$\begin{aligned}
 \chi_{\text{CH}_4,\text{a},0} &= 1/3.5, \chi_{\text{H}_2\text{O},\text{a},0} = 2.5/3.5, \chi_{\text{H}_2\text{O},\text{c},0} = 0.2, \chi_{\text{CO}_2,\text{c},0} = 0.1, \\
 \chi_{\text{O}_2,\text{c},0} &= 0.1, \chi_{\text{N}_2,\text{c},0} = 0.6, \theta_{\text{a},0} = 3, \theta_{\text{c},0} = 3, \\
 \theta_{\text{m},0} &= 3, \theta_{\text{s},0} = 3.1, \gamma_{\text{a},0} = 1, \gamma_{\text{c},0} = 6, \\
 \Phi_{\text{a},0}^{\text{S}} &= 32.3, \Phi_{\text{c},0}^{\text{S}} = 32.3, U_{\text{cell},0} = 32.3, \chi_{\text{H}_2\text{O},\text{m},0} = 0.2, \\
 \chi_{\text{CO}_2,\text{m},0} &= 0.1, \chi_{\text{O}_2,\text{m},0} = 0.1, \chi_{\text{N}_2,\text{m},0} = 0.6.
 \end{aligned}$$

3 Numerical Methods and Results

A widely used idea is to transform partial differential equations into a system of ordinary differential algebraic equations by discretizing the model functions subject to the spatial variable z . This approach is known as the numerical method of lines (MOL), see for example Schiesser [12]. We define a uniform grid of size n_g and get a discretization of the whole space interval from $z = 0$ to $z = 1$. To approximate the first and second partial derivatives of the state variables subject to the spatial variable at a given point z_k , $k = 1, \dots, n_g$, several different alternatives have been implemented in the code PDEFIT, see Schittkowski [14] for more details, which is applied for the numerical tests of this paper.

Spatial derivatives of the heat variable $\theta_s(z, t)$ are approximated by a three-point-difference formulae for first derivatives, which is recursively applied to get second derivative approximations. The difference formulae are adapted at the boundary to accept given function and gradient values. First derivatives of the remaining transport variables are approximated by simple forward and backward differences, so-called upwind formulae, where the wind direction is known in advance. Ordinary differential and algebraic equations are added to the discretized system without any further modification.

In case of algebraic partial or ordinary differential equations, boundary conditions have to satisfy the algebraic equations. Consistent initial values are computed internally proceeding from given starting values for the nonlinear programming algorithm NLPQL of Schittkowski [13]. It is known that the system of PDAEs possesses the index one.

The method of lines leads to a large system of differential algebraic equations, where the size depends on the number of grid points, i.e., on n_g . The system equations are integrated by the implicit code RADAU5, see Hairer and Wanner [6]. Because of the non-continuous input variable

$$I_{\text{cell}}(t) := \begin{cases} 3, & \text{if } t \leq 1000 \\ 3.5, & \text{if } t > 1000 \end{cases} ,$$

the cell current, the right-hand side of some equations become non-continuous subject to integration time. Thus, it is necessary to restart the integration of the DAE at $t = 1000$.

Because of a complex input structure, the code PDEFIT is called from a GUI called EASY-FIT, see Schittkowski [15, 16], to facilitate modeling, execution, and interpretation of results. Model functions are interpreted based on a language called PCOMP similar to Fortran, see Schittkowski [17]. To give an example, consider the parabolic heat equation which is implemented in the form

```
*      FUNCTION Ts_t
      sigmaTred = (-hrred + nred *(phicS - phicL))*Dared*rred
      sigmaTox  = (-hrox1 + nox1*(phiaS - phiaL))*Daox1*rox1
      /          + (-hrox2 + nox2*(phiaS - phiaL))*Daox2*rox2
      qsolid   = sigmaTox + sigmaTred - (phicL - phiaL)/F
      hsc      = cpm*(-ncsC02 - ncs02)*(Tc - Ts)
      hsa      = cpm*(-nasH2 - nasC02)*(Ta - Ts)
      qcond    = Ts_zz*12/Pes
      Ts_t     = (qcond + hsa + hsc - qas - qcs + qsolid)/cps
```

Here, Ts_zz denotes the second partial derivative of $\theta_s(z, t)$ subject to the spatial variable z .

The MOL is applied with $n_g = 15$ lines. For our numerical tests, the absolute stopping tolerance of RADAU5 is $\epsilon = 10^{-5}$. The DAE is integrated from $t = 0$ to $t = 2000$ with a break at $t = 1000$.

The numerical solution of some selected components is shown in Figures 2–13 to illustrate the qualitative behavior of the state variables.

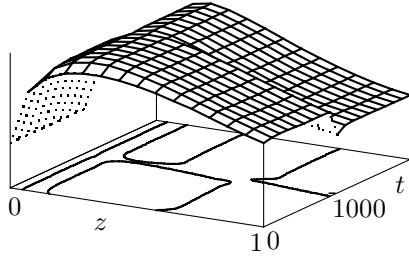


Fig. 4. Molar fraction $\chi_{\text{H}_2,\text{a}}$ in anode gas channel

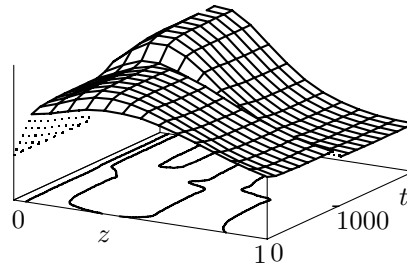


Fig. 5. Molar fraction $\chi_{\text{CO},\text{a}}$ in anode gas channel

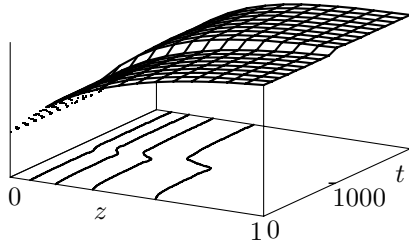


Fig. 6. Molar fraction $\chi_{\text{CO}_2,\text{a}}$ in anode gas channel

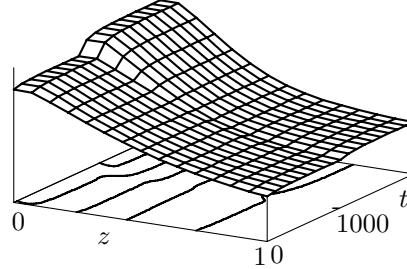


Fig. 7. Molar fraction $\chi_{\text{H}_2\text{O},\text{c}}$ in cathode gas channel

Note that at $t \approx 800$ the stationary solution for $I_{\text{cell}} = 0.3$ is reached. At $t = 1000$ the load change happens. At $t \approx 1800$ the new stationary solution for $I_{\text{cell}} = 0.35$ is reached. The molar fraction of methane and water depicted in Figures 2 and 3 decrease over the entire spatial width due to the methane and water consuming endothermic reforming reaction. In accordance with the methane behavior, hydrogen is produced in the endothermic reforming reaction immediately after the anode inlet, to become subsequently consumed in the exothermic oxidation reaction, see Figure 4. At $t = 1000$ the load change takes place. More electrons are needed, therefore due to (ox1) the molar fraction of hydrogen decreases (Fig. 4). In Figures 5 and 6, the behavior of the molar fractions of carbon monoxide and dioxide are plotted. The molar fraction of water increases in flow direction of the cathode gas channel, Figure 7, whereas the molar fractions of carbon dioxide and oxygen decrease, see Figures 8 and 9.

The most important results concern the temperatures shown in Figures 10 to 11. They directly influence the reaction rates. Moreover, the solid temperature of Figure 12 must be particularly observed to avoid so-called hot spots leading to material corrosion and consequently to a reduced service life. The temperature distribution in the anode channel coincides with the heat demand and the heat release of the reactions therein, see Figure 10. Initially we

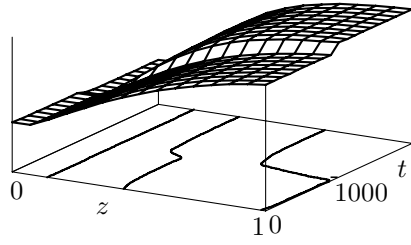


Fig. 8. Molar fraction $\chi_{\text{CO}_2,c}$ in cathode gas channel

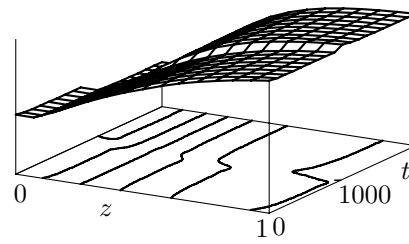


Fig. 9. Molar fraction $\chi_{\text{O}_2,c}$ in cathode gas channel

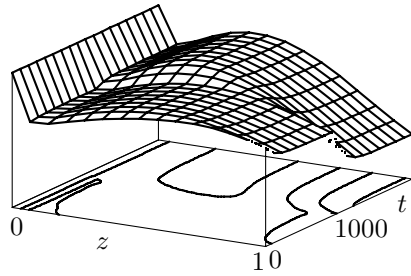


Fig. 10. Temperature θ_a in anode gas channel

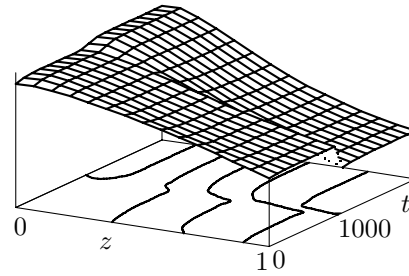


Fig. 11. Temperature θ_c in cathode gas channel

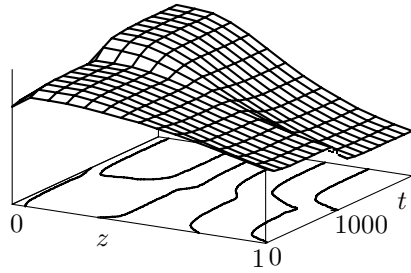


Fig. 12. Temperature θ_s in solid

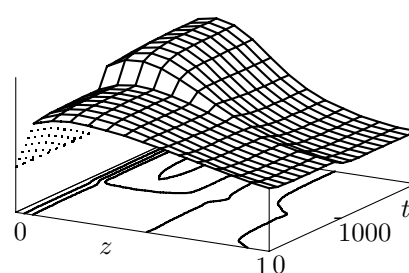


Fig. 13. Current density i_a

have the endothermic reforming reaction and thus, the temperature declines. Subsequently, the anode gas temperature is increased again by heat exchange with the solid, which is heated by the electro chemical reactions. Since the cathode gas is heated up by the solid phase along the channel, the temperature continuously increases, see Figure 11. Finally, the current density i_a is plotted in Figure 13. i_a is almost similar to i_e and i_c .

4 Conclusions

A complex mathematical model describing realistically the dynamical behavior of a molten carbonate fuel cell, has been presented. The semi-discretisation in space of the large scale partial differential-algebraic equation system together with its nonstandard boundary conditions including an Integro-DAE system yields a large system of differential-algebraic equations by the method of lines. The obtained numerical results correspond to the practical experiences of engineers with real fuel cells of the type investigated. The model will be used in future for optimal boundary control purposes.

Acknowledgments

The research project was partly funded by the German Federal Ministry of Education and Research within the WING-project "Optimierte Prozessführung von Brennstoffzellensystemen mit Methoden der Nichtlinearen Dynamik". We are indebted to Dr.-Ing. P. Heidebrecht and Prof. Dr.-Ing. K. Sundmacher from the Max-Planck-Institut für Dynamik Komplexer Technischer Systeme, Magdeburg, for providing us with the fuel cell model, to Dr. K. Sternberg from the University of Bayreuth for her advice and to Dipl.-Ing. J. Berndt and Dipl.-Ing. M. Koch from the management of IPF Heizkraftwerksbetriebsges. mbH, Magdeburg, for their support.

References

1. M. Bauer, *1D-Modellierung und Simulation des dynamischen Verhaltens einer Schmelzcarbonatbrennstoffzelle*, Diplomarbeit, Universität Bayreuth, 2006.
2. M. Bischoff, G. Huppmann, *Operating Experience with a 250 kW_{el} Molten Carbonate Fuel Cell (MCFC) Power Plant*, *Journal of Power Sources*, **105**, 2 (2002), 216–221.
3. K. Chudej, P. Heidebrecht, V. Petzet, S. Scherdel, K. Schittkowski, H.J. Pesch, K. Sundmacher, *Index Analysis and Numerical Solution of a Large Scale Non-linear PDAE System Describing the Dynamical Behaviour of Molten Carbonate Fuel Cells*, *Z. angew. Math. Mech.*, **85**, 2 (2005), 132–140.
4. K. Chudej, K. Sternberg, H.J. Pesch, *Simulation and Optimal Control of Molten Carbonate Fuel Cells*, In: I. Troch, F. Breitenecker (Eds.), *Proceedings 5th Mathmod Vienna*, Argesim Report No. 30, Argesim Verlag, Wien, 2006.
5. M. Gundermann, P. Heidebrecht, K. Sundmacher, *Validation of a Mathematical Model Using an Industrial MCFC Plant*, *Journal of Fuel Cell Science and Technology* **3** (2006), 303-307.
6. E. Hairer, G. Wanner, *Solving Ordinary Differential Equations II, Stiff and Differential-Algebraic Problems*, Springer, Berlin, 1996, 2nd. rev. ed.
7. P. Heidebrecht, *Modelling, Analysis and Optimisation of a Molten Carbonate Fuel Cell with Direct Internal Reforming (DIR-MCFC)*, VDI Fortschritt Berichte, Reihe 3, Nr. 826, VDI Verlag, Düsseldorf, 2005.

8. P. Heidebrecht, K. Sundmacher, *Dynamic Modeling and Simulation of a Countercurrent Molten Carbonate Fuel Cell (MCFC) with Internal Reforming*, Fuel Cells **3–4** (2002), 166–180.
9. P. Heidebrecht, K. Sundmacher, *Molten carbonate fuel cell (MCFC) with internal reforming: model-based analysis of cell dynamics*, Chemical Engineering Science **58** (2003), 1029–1036.
10. P. Heidebrecht, K. Sundmacher, *Dynamic Model of a Cross-Flow Molten Carbonate Fuel Cell with Direct Internal Reforming*. Journal of the Electrochemical Society, **152** (2005), A2217–A2228.
11. S. Rolf, *Betriebs Erfahrungen mit dem MTU Hot Module*, In: Stationäre Brennstoffzellenanlagen, Markteinführung, VDI Berichte, Nr. 1596, VDI Verlag, Düsseldorf, 2001, 49–57.
12. W.E. Schiesser, *The Numerical Method of Lines*, Academic Press, New York, London, 1991.
13. K. Schittkowski, *NLPQL: A FORTRAN Subroutine Solving Constrained Nonlinear Programming Problems*, Annals of Operations Research, **5** (1985/86), 485–500.
14. K. Schittkowski, *PDEFIT: A FORTRAN code for parameter estimation in partial differential equations*, Optimization Methods and Software, **10** (1999), 539–582.
15. K. Schittkowski, *Numerical Data Fitting in Dynamical Systems - A Practical Introduction with Applications and Software*, Kluwer Academic Publishers, Dordrecht, Boston, London, 2002.
16. K. Schittkowski, *EASY-FIT: A Software System for Data Fitting in Dynamic Systems*, Structural and Multidisciplinary Optimization, **23** (2002), 153–169.
17. K. Schittkowski, *PCOMP: A Modeling Language for Nonlinear Programs with Automatic Differentiation*, in: Modeling Languages in Mathematical Optimization, J. Kallrath ed., Kluwer Academic Publishers, 2004, 349–367.
18. K. Schittkowski, *Data Fitting in Partial Differential Algebraic Equations: Some Academic and Industrial Applications*, Journal of Computational and Applied Mathematics **163** (2004), 29–57.
19. W. Winkler, *Brennstoffzellenanlagen*, Springer, Berlin, 2002.